

Preparation and Characterization of Poly(2-Hydroxyethyl Methacrylate) Grafted Bacterial Cellulose Using Atom Transfer Radical Polymerization

Bohdan Volynets, Hamza Nakhoda, Mustafa Abu Ghalia, and Yaser Dahman*

Department of Chemical Engineering, Ryerson University, Toront M5B 2K3, Canada
(Received November 7, 2016; Revised February 26, 2017; Accepted March 4, 2017)

Abstract: The purpose of this study is to synthesize grafted Bacterial Cellulose (BC) nanofibers using Atom Transfer Radical Polymerization (ATRP) reinforced into poly(2-hydroxyethyl methacrylate) (PHEMA) hydrogel matrix. Nanofibers grafting polymerizations were conducted in the presence of the catalyst CuCl/CuBr and the initiator 2-bromoisobutyrylbromide (2-BiBr). Degrees of substitution (DS) of BC-macroinitiators were quantified using both elemental analysis and gravimetric method. FTIR results confirmed BC nanofibers' surface modifications of both initiator and hydroxyethyl methacrylate (HEMA) grafts. X-ray spectroscopy further confirmed the increase in carbonyl content after PHEMA-grafting polymerization. Results of the gravimetric analysis showed an increase in the weight of the grafted BC upon increasing reaction time. Furthermore, the change in the swelling ratio percentages of the reinforced composites product (BC-MI-3-g-PHEMA-1.5) was considerably higher based on reaction time. Slight increase in the swelling ratio of BC-MI-3 nanofibers was observed after 48 hours to reach 31 %. Moreover, results of thermal gravimetric analysis (TGA) demonstrated that decomposition temperature at 50 % weight loss (T_{50}) decreased to 350 °C for BC-MI-3-g-PHEMA-1.5. These characteristics demonstrate potentials for applications in the biomedical fields including drug delivery and wound care.

Keywords: Bacterial cellulose, Nanofibers grafting, Atom transfer radical polymerization, Macroinitiator

Introduction

As previous studies have shown, 2-hydroxyethyl methacrylate (HEMA) is polymerized using different methods such as free radical [1], anionic [2], and controlled/living polymerization [2-4]. For many years, free radical polymerization has been the simplest and most widely used technique on an industrial scale. This is due to the simple radical generation and the applicability to various monomers containing different functional groups [3]. In addition to homo- or block polymerizations of HEMA, Robinson *et al.* [4] studied the high efficient controlled polymerization of HEMA by ATRP in methanol/water mixtures. Reining *et al.* [5] investigated the formation of HEMA via ATRP as a block copolymer. This is comprised of a poly(ethylene oxide) (PEO) macro-initiator in ethylene glycol where their polymerization proceeded in a controllable gradient to high monomer conversions. Recently, Malmstrom and Carlmark [2], prepared HEMA via ATRP at different temperatures of 50 and 70 °C using CuCl as a catalyst in a 70:30 methyl ethyl ketone (MEK)/n-propanol mixed solvent. However, results reported of polymerization had poor living characteristics. Despite the previous studies, cellulose grafted PHEMA polymerization in a solvent has not been studied sufficiently. Cellulose-graft-PHEMA copolymers can be useful in drug delivery applications because of their biocompatibility and biodegradability. Over the past decade, the modification of cellulose for developing new material such as hydrogel has received increasing attention [2,6]. This is because cellulose is one of the most abundant polymers found naturally on earth; it can be found in plant cell walls and also

can be produced by bacterial strains of *Gluconacetobacter xylinus*. BC nanofibers are less than 50 nm in diameter and highly crystalline, being made up of a bundle of cellulose microfibrils that in turn consist of semi-crystalline cellulose chains. The Young's modulus and tensile strength of BC nanofibers are around 138 GPa and 2 GPa respectively, which is comparable to those of high strength aramid fibers. The thermal expansion coefficient in the axial direction is as small as $0.1 \times 10^{-6} \text{ K}^{-1}$. These remarkable properties for BC nanofibers make them an excellent material for engineering high strength composites [7-9]. Recently, Atom Transfer Radical Polymerization (ATRP) has been one of the most studied among controlled radical polymerization techniques. Wang and Matyjaszewski [10] in addition to Kato *et al.* [11] used copper based catalysts for ATRP that was conducted with a halogen as the transferable atom. This polymerization was further developed by Boutevin [12] through an additional reaction in which a transition metal catalyst acted as a carrier of the halogen atom in a reversible redox process [13].

Controlled polymerization techniques such as ATRP and reversible addition fragmentation chain transfer (RAFT) polymerization are particularly attractive for the preparation of polymers with narrow polydispersity and controlled molecular weight. They offer control over chain-ends so their reactions are described as controlled/"living" polymerization. In the "grafting from" approach, polymerization is directly initiated from initiator-functionalized or an RAFT-agent functionalized surface [14]. Hence, surface initiated controlled/living radical polymerization is a versatile and powerful technique. It can be used for surface modification of various substrates such as gold, silicon wafers, carbon nanotubes, and polymer membranes [15]. The most extensively used

*Corresponding author: ydahman@ryerson.ca

modification technique involves a covalent graft polymerization method that occurs in two forms: “grafting to” and “grafting from” for membrane coatings. However, the “grafting from” approach is preferable because it enables a higher graft density while still preserving control over the polymer architecture and coating thickness. In a previous study, Dahman and Oktem [16] successfully grafted PHEMA onto BC nanofibers using free radical polymerization with prior acetylation. However, free radical polymerization is known to provide little control over the structure of polymer grafts. In the present work, PHEMA was grafted onto BC by ATRP to attain better control over the grafted polymer chain.

Experimental

Materials

All the following chemicals were purchased from Sigma-Aldrich and used as received: 2-hydroxyethyl methacrylate (HEMA), 2-bromoisobutyl bromide (2-BiBr) as initiator, tetrahydrofuran (THF), pyridine 99.8 % anhydrous, 2,2'-bipyridyl (bpy), catalyst CuCl, CuBr₂ 99 %, BC nanofibers were produced using the bacterial strain *Acetobacter xylinus* BPR2001, which was purchased from American Type Culture Collection (ATCC).

Synthesis Nanostructure Biomaterials

Nanostructured biocomposites samples were synthesized through the following three main steps: Synthesis of BC Nanofibers, surface modification of BC nanofibers, and grafting of PHEMA on the surface of the nanofibers.

Synthesis of BC Nanofibers

Green BC nanofibers were produced via Separate Hydrolysis and Fermentation (SHF), depending solely on the renewable resources of agricultural residues as feedstock. Wheat straw was used as the fermentation carbon source where it was pre-treated with 1 % diluted sulfuric acid. Resultant hydrolysate solution was adjusted to the proper fermentation conditions and then inoculated with *Acetobacter xylinus* bacteria. The course of BC fermentation production lasted for 7 days. The solution was then treated with excess NaOH at 100 °C for cell lysis. Five runs of repeated washing and centrifugation extracted the produced nanofibers. Stock solutions of the BC nanofibers were stored as a suspension solution with a concentration of 42 g/l [9].

Synthesis of the Macro-Initiator BC-Br

BC nanofibers were transferred into THF by a stepwise solvent exchange (water-methanol-acetone-THF). In 125 ml round bottom flask, 1 ml of pyridine was added to 25.2 mg of BC in 35 ml of THF and then cooled in ice under stirring. 0.22-0.89 ml (50-200 mM) of 2-bromoisobutyl bromide was diluted in 5 ml THF and cooled in ice prior the dropwise addition to the reaction flask. The reaction mixture was

left under stirring at room temperature for 2 hours. Finally, the mixture was washed with deionised water, and the obtained BC macro-initiator was stored at room temperature in deionised water until further use.

Graft Copolymerization of HEMA onto BC Macroinitiator

The grafting technique was conducted according to the procedures outlined in the literature [17]. Copolymerization of HEMA monomers onto BC macroinitiator in 15 ml of H₂O (50 vol %) and 15 ml of HEMA were mixed in the presence of a catalyst of 55 mg (3.05 mmol) of CuCl, 36 mg (1.98 mmol) of CuBr₂, and 244 mg (13.54 mmol) of bpy were added while continuously stirring BC in the reactor under N₂ atmosphere. All grafting experiments were conducted on BC nanofibers of the degree of substitution (DS) ~1. An aqueous suspension of BC macroinitiator with a known concentration was transferred to 200 ml of THF by the stepwise solvent exchange. The polymerizing reactor was conducted in a 500-ml glass vessel equipped with a reflux condenser and stirring speed of 300 rpm through a pitched blade impeller fixed to a shaft (Heidolph PR 30 and 39; Schwabach, Germany). Heidolph PR 30 and 39 had propeller diameters of 58 mm and 75 mm, respectively, and were driven by a Heidolph RZR 2020 motor. The initiator was allowed to interact with the BC macroinitiator for 15 min at 60 °C using an oil bath, followed by the addition of HEMA monomers of required initial weight (200 % w/w). Atomic Transfer Radical Polymerization was continued for 6 hours at 60 °C under nitrogen. Sample BC-g-PHEMA-2.0 (2 % w/w monomer to cellulose ratio, Table 4) was the reinforcing element at different initial concentrations of 0.5, 1.0, 1.5, and 20 % (w/w) with respect to the HEMA monomer. The final product was molded in the form of sheets of few millimeters thickness.

Analytical Methods

SEM/EDS Analysis

Scanning electron microscopy (SEM) and energy dispersive X-ray spectroscopy (EDS) analyses were performed to characterize functionality and grafting of the nanofibers. The samples were vacuum dried on aluminum SEM holders and analyzed by JEOL/OE equipment model JSM-6380 LV (Oxford Instrument, UK-software version SEI England) with a monochromator (Al X-ray source) to avoid charging on the surface. All nanofiber samples were sputter coated with a conductive layer of gold (5-7 nm). The samples were then analyzed with a magnification of ×10k for cellulose nanofibers. The SEM with an acceleration voltage of 2 kV beam voltage was used on less than 1 mm² to ensure a higher surface sensitivity of the polymer fibers and to generate high-resolution images.

Gravimetric Measurement

The gravimetric analysis method was conducted to quantify the change in BC nanofibers weights due to grafting with

PHEMA. The percentages of grafting for different samples (G%) were quantified as the weight of BC grafted with PHEMA relative to the weight of BC macroinitiator, as listed in Table 4. Weights of the nanofibers were measured using a high precision scale (0.0001 g precision). All samples were dried at 80 °C for 24 hours in an oven until constant weight was obtained (no moisture content) before taking weight measurements.

Fourier Transform Infrared Spectroscopy (FTIR)

The surface of macroinitiator samples was examined by ATR-FTIR (Attenuated Total Reflectance Fourier Transform Infrared spectroscopy). Nicolet Nexus 8700 FTIR Spectrophotometer (Thermo Electron Corporation) was fitted with a "Smart Orbit" Attenuated Total Reflectance (ATR) accessory containing a diamond crystal internal reflection element with a resolution of 4 cm⁻¹, the number of scans 64, and mirror velocity of 0.6329 cm⁻¹. Macroinitiator samples were placed active face down on the ATR crystal and held in place by a clamp. FTIR spectra were recorded in 5 individual scans at 2 cm⁻¹ resolutions in the 500–4000 cm⁻¹ interval.

Swellability Measurements

The swelling ratio (SR) of the BC-g-PHEMA was measured using the weights method (before and after immersion in water) [18]. Specimens (dimensions of 1×1 cm) were immersed in distilled water at room temperature to study swelling at a minimum of three samples (tested for each material). The weight increase was periodically assessed for 2 days. Samples were taken out of the water and the wet surfaces were immediately wiped with dry filter paper and then re-immersed. Then the SR was calculated using equation [19].

$$SR(\%) = \frac{(W_S - W_D)}{W_D} \times 100 \quad (1)$$

where W_D is the initial weight of the dry film and W_S is the weight of the water-swollen film.

Thermal Gravimetric Analysis

Thermal gravimetric analysis (TGA) was performed to study the thermal degradation behavior of the nanocomposites samples. The TGA was carried out using Shimadzu TGA 50 analyzer equipped with the platinum cell. All samples were heated at a constant rate of 10 °C/min from room temperature to 600 °C. This was conducted on 10 mg of each sample under a nitrogen flow of 20 ml/min. Thermal stability factors, including initial decomposition temperatures (T_{onset}), the temperature of maximum rate of degradation (T_{max}) and decomposition temperature at 50 % weight loss (T_{50}) of the BC macroinitiator (BC-MI-3) and its grafted samples at different reaction times was determined from the TGA.

Results and Discussion

Figure 1 summarizes the reaction mechanism of BC nanofiber-based macroinitiator and BC grafted-PHEMA. The BC nanofiber macroinitiators with different numbers

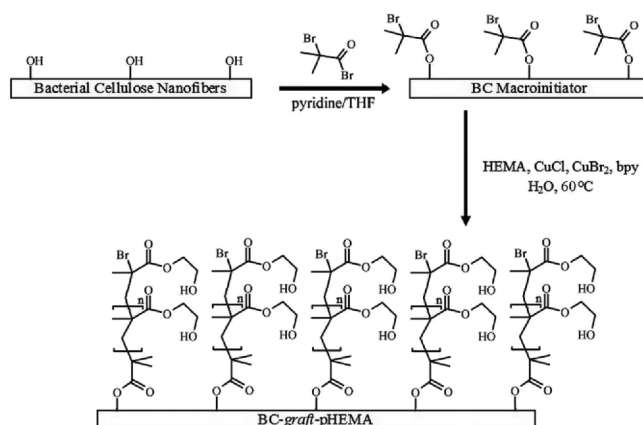


Figure 1. Reaction scheme representing BC nanofibers surface functionalization and grafting.

of initiating sites were synthesized by direct acylation of BC nanofiber. According to the reaction mechanism, the macroinitiator BC-Br was used to initiate the polymerization of HEMA on the BC nanofiber hydroxyl groups using 2-BiBr in the presence of THF/Pyd mixture [20–23]. Subsequently, the HEMA was grafted on the BC nanofibers using CuCl, CuBr₂, bpy H₂O at 60 °C. The amount of initiator has significant effect to form BC-graft-PHEMA with a considerable weight gain resulting from PHEMA grafting. The grafting of PHEMA chains on the BC macroinitiator led to substantial changes on the degree of substitution of macroinitiator [23].

SEM images in Figure 2 demonstrates that the diameter of BC nanofiber is comparatively small as compared to their length, indicating that the BC nanofibers are of high aspect ratios. Nonetheless, the BC after being polymerized by PHEMA displays different fibers orientations and relatively smooth surface (polymerized PHEMA). In addition, the SEM images revealed that the nanofibers are interacted at the interfacial area, and therefore are exhibited entirely different in dispersion from the original BC nanofibers [23, 24].

Grafting reaction parameters on the surface of BC using ATRP were analyzed in this study. An experiment was designed to investigate the effect of the concentration of 2-BiBr on the degree of substitution of OH groups in BC. The reaction time was chosen as 2 hours to ensure efficient mixing. The concentration of 2-BiBr was chosen to be in the range of 0 to 200 mM using 50 mM increments. Upon washing with water, it was found that all samples formed a suspension in water. The sample that had 200 mM of 2-BiBr agglomerated. The samples were subjected to SEM/EDS analysis in an attempt to quantify the degree of substitution of 2-BiBr [25].

The effects of x-ray electron dispersive spectroscopy are presented in Table 1. In general, the % elemental bromine increased as the concentration of 2-BiBr increased. The samples were transferred into THF by the stage-wise solvent

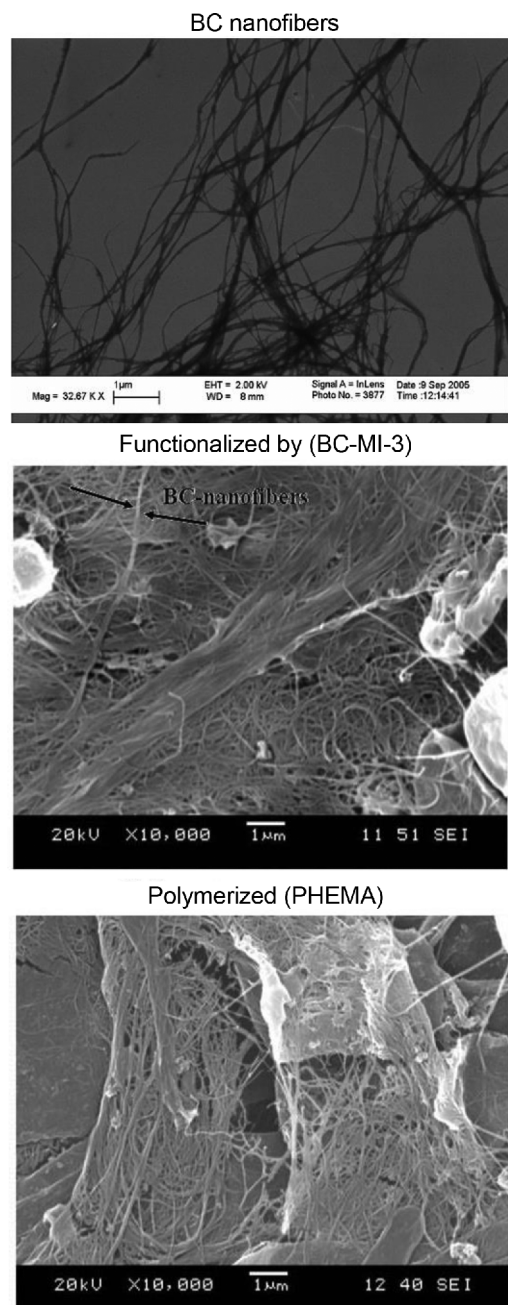


Figure 2. SEM images of BC macroinitiator (BC-MI-3) and grafted BC nanofibers (BC-MI-3-g-PHEMA) (magnification of $\times 10k$).

Table 1. EDS elemental analyses results of BC macroinitiators BC-MI-n (n:1-4) prepared at different 2-BiBr concentrations at room temperature

Sample ID	Reaction time (h)	BC (mg)	Amount of 2-BiBr		Pyridine (ml)	THF (ml)	C	O	Br (%)	DS
			(ml)	(mM)						
BC	-	-	-	-	-	-	53.26	46.74	-	-
BC-MI-1	2	25.2	0.223	50	1	35	55.07	44.80	0.14	0.04
BC-MI-2	2	25.2	0.470	100	1	35	55.76	44.02	0.19	0.05
BC-MI-3	2	25.2	0.668	150	1	35	55.28	44.63	0.10	0.03
BC-MI-4	2	25.2	0.890	200	1	35	56.96	41.79	1.26	0.35

exchange. The sharp deviation of elemental Br percentage from the sample BC-MI-3 (from 0.19 to 0.10 % Br) may be due to the insufficient water removal during the process. This can be related to the competition between water and hydroxyl groups that impacts the esterification reaction with 2-BiBr in the aforementioned reaction scheme. The solvent exchange was the only factor overlooked in this experiment. DS was calculated using equation (2) below. Mainly, this equation is the inverse of equation (3) that represents the elemental bromine content (%Br). Results for DS are summarized in Table 1.

$$DS = \frac{11\%BrMPF}{MS(100-6\%Br)} \quad (2)$$

$$\%Br = \frac{100 \times MS \times DS}{MPF(6+5) + 6MS \times DS} \quad (3)$$

where DS is the degree of substitution, MPF is the number of cellulose chains per fiber and MS is the number of cellulose chains on the fiber surface. In order to evaluate some of the parameters is equation (2), a number of BC nanofibers bundle have been characterized by x-ray electron dispersive spectroscopy. Diameter of BC nanofibers bundles were in the range of 50-60 nm, and the cross-sectional area occupied by a BC nanofiber bundle in the crystal lattice of 0.317 nm². Accordingly, the scale up would be to have 1000 cellulose chains with total MPF of 400 on the surface per each fiber (MS). With a length of one cellulose molecule, there are 1200 OH groups on the surface [26].

Figure 3 shows the EDS survey spectrum of BC-MI-3, where the large peaks observed at 529 eV and 285 eV correspond to oxygen 1 s and carbon 1 s, respectively. Whereas the small peak that is hardly visible at 70 eV corresponds to bromine 3d [26]. The presence of this peak was ascertained by a high-resolution scan in the bromine 3d region, as shown in the inset of Figure 3. The previous finding confirms the binding of bromo-initiator to BC nanofibers [27].

Figure 4 illustrates that elemental bromine content percentage increased rapidly with the increase in 2-BiBr concentration. However, the degree of substitution appeared to decrease sharply at 150 mM of 2-BiBr to reach 10 % Br. This was attributed to the effect of many parameters such as temperature, solubility, and water removed from 2-BiBr during

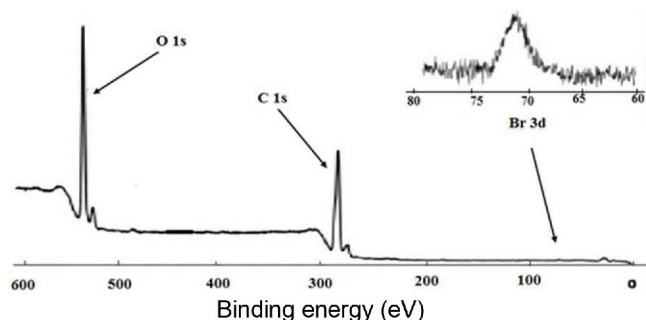


Figure 3. EDS survey spectrum scan of BC macroinitiator (BC-MI-3) with inset showing high resolution Br-3d.

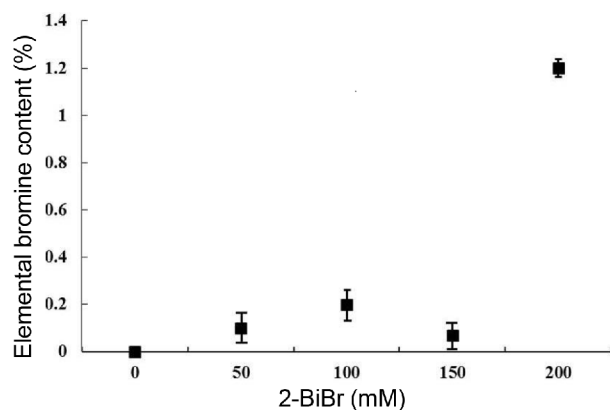


Figure 4. Change in elemental bromine content percentage at different concentrations of 2-BiBr.

the reaction processes. The literature data for surface modification of BC nanofibers demonstrates that there is a linear relationship between the concentration of 2-BiBr used for BC functionalization and the degree of substitution related to the bromine element content [27]. In the present study, the same linear relationship was obtained when 2-bromoisobutyryl bromide was reacted with BC. With a molecular weight of 229.9 g/mole, compared to the molecular weight of acetic anhydride of 102.09 g/mole, 2-BiBr molecule is more bulky. Its penetration into the core of BC nanofibers would be less favorable or limited, especially for amorphous regions of the cellulose. Further experimental research is required to investigate the dynamic reaction of 2-bromoisobutyryl bromide with BC nanofibers. Also, the 2-bromoisobutyryloxy group contains more carbon than oxygen. Therefore substitution of 2-bromoisobutyryl bromide on the surface should result in an increase in elemental carbon and a decrease in elemental oxygen; see Table 1. This observation indicated that this change may have corresponded to confirm the immobilization of the initiator on BC nanofibers. Carlmark and Malmstrom [19] used electron spectroscopy (ESCA) to analyze different patches of BC that were treated with 2-bromoisobutyryl bromide. They observed that when a new

Table 2. Synthetic parameters of two samples of BC macroinitiators at two different concentrations of 2-BiBr

Sample ID	Time (h)	BC (mg)	Total volume (in THF) (ml)	Pyridine (ml)	2-BiBr Concentration	
					(mM)	(ml)
BC-MI-2	2	4.0	200	12.5	400	10
BC-MI-3	2	4.0	200	12.5	200	5

batch of BC contained larger BC shredded (i.e., particles), a shift occurred in the concentration of 2-BiBr, required to increase BC hydrophobicity. Results in Table 2 demonstrate that BC macroinitiator remained hydrophilic and formed a suspension in water at a concentration of 200 mM of 2-BiBr. At 400 mM of 2-BiBr, BC macroinitiator was hydrophobic and formed spherical clumps in water. Results from EDS demonstrated that BC-MI-3 has low DS of ~0.03 as a result of low percentage of Br element, and therefore possess fewer OH groups. Meanwhile, BC-MI-4 shows an increase in DS to ~0.35, which demonstrated more OH groups have been esterified to form BC-macroinitiator. These results are consistent with Shen and Huang [28] who initiated BiBBr to cellulose diacetate in solution prior to grafting with poly(methyl methacrylate) (PMMA). They also reported a decline in the concentration of OH groups upon higher amount of initiator used.

The formation of BC macroinitiator (BC-MI-3) and its grafting with PHEMA were confirmed by FTIR in Figure 5. This was demonstrated by the carbonyl ester group stretching band of the 2-bromoisobutyrate group at 1730 cm^{-1} (see Table 3). This doesn't appear in the control spectrum of the BC nanofiber. Moreover, the intensity of this corresponding (C-O ester) band increased in the spectrum of BC-MI-3-g-PHEMA than that in BC-MI-3 (Figure 5(A)), confirming the increase in the degree of substitution. Symmetric C-H stretching vibrations for C-H group was corresponding at 2830 cm^{-1} . The sharp peak at 3380 cm^{-1} in the spectra of BC-MI-3-g-PHEMA is confirming the presence of hydroxyl group. It is also clear that there is no significant shift in carbonyl group band, as observed by the pristine BC. Moreover, the appearance of stretching band of (C-O) ester group in the range of 1000-1200 cm^{-1} in the spectrum of BC-MI-3-g-PHEMA, is another evidence for the involvement of HEMA in polymerization reaction on the surface of BC-MI-3 [29]. Studies for the substitution of 2-bromoisobutyryl bromide on cellulose fibers, done by Carlmark and Malmstrom [19] reported the failure of analyzing full substitution of the hydroxyl using FTIR was due to the layer of Bromo-ester groups was very thin. In compared to the ATR-FTIR measurement that utilizes thickness on the micrometer scale. On the other hand, Gang *et al.* [30] reported band intensity increase in alpha-bromo substituted carbonyl stretching at 1730 cm^{-1} , as reaction time increase. This work was conducted on cotton

fibers (structurally contains cellulose repeated units) subjected to a reaction with 2-bromoisobutryl bromide. This finding matches the current study as described in Figure 5(A).

Similarly, the FTIR spectra for both initiators BC-MI-2

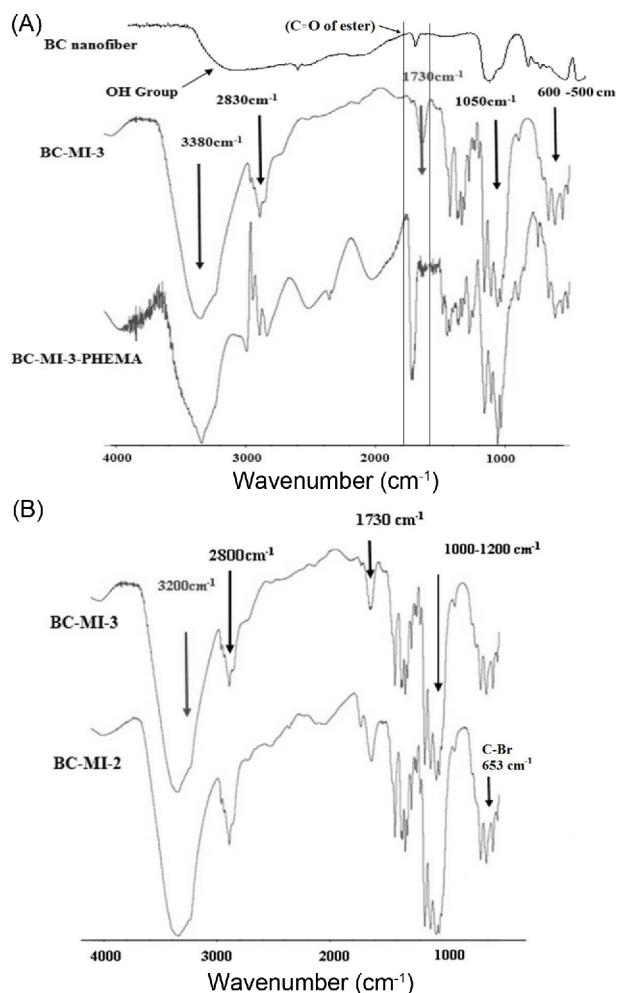


Figure 5. (A) FTIR spectra of free BC nanofibers, BC macroinitiator (BC-MI-3) and BC grafted with PHEMA (BC-MI-3-PHEMA) and (B) FTIR spectra of two BC macroinitiators samples (i.e., BC-MI-2 and BC-MI-3) that were prepared at different 2-BiBr concentrations of 200 mM and 400 mM, respectively.

Table 3. FTIR peak assignments as arose in Figures 5 and 6

Functional group	Experimental (cm ⁻¹)	Book [29] (cm ⁻¹)	Paper [28] (cm ⁻¹)
vC=O (ester)	1730	1730-1750	1720
vC-H (alkanes)	2800-2830	2850-3000	-
vC-O (ester, ether)	1000-1200	1000-1300	1200
vO-H (alcohols)	3200-3380	3200-3650	3320
vC-Br	500-600	<667	550

and BC-MI-3 in Figure 5(B) showed four characteristic bands at 3200, 2800, 1730, 1000 and 500 cm⁻¹. These peaks are assigned to the stretching of hydroxyl O-H, C-H, C=O, C-O and C-Br, respectively. As seen in Figures 5(B) and 6, BC-MI-2 spectrum showed a clear increase in C=O stretch at 1730 cm⁻¹ compared to the macroinitiator that was synthesized using concentration twice as low as that of 2-BiBr. Furthermore, the spectrum of BC-MI-3-g-PHEMA showed a drastic increase in C=O stretching at 1730 cm⁻¹. This was due to the grafting of BC with PHEMA for 1 hour compared to the BC macroinitiator used to initiate the grafting.

Results of the gravimetric analysis are illustrated in Figure 6 as well as in Table 4. Examining Figure 6 reveals the percentage of weight increment over time of BC macroinitiator due to grafting by PHEMA relative to the weight of unreacted BC macroinitiator. Table 4 summarizes results for the change in the weight of BC nanofibers, grafted with PHEMA relative to the weight of BC macroinitiator. At similar conditions and parameters of grafting, results in Table 4 demonstrates that the increase in reaction times resulted in increasing values of nanofibers' grafting percentages.

Table 4 summarizes changes in weight percentages of BC grafted-PHEMA at different reaction times. Results in Table 4 shows that weight of BC grafted with PHEMA relative to the weight of unreacted BC macroinitiator (G%) increased with the increase in reaction time. This represents higher yield obtained up to ~153.3 % with higher reaction time of 1.5 hours. Alternatively, in a previous work by Pulat *et al.* [31], they confirmed that the growing polymer chains via uncontrolled free radical polymerization have resulted in termination reactions after short period of time. Consequently, grafting yield of HEMA obtained was as low as 47.6 % after 2 hours.

Figure 6 demonstrates the change in weight percentage of grafted BC nanofibers (BC-MI-3-g-PHEMA) as a function

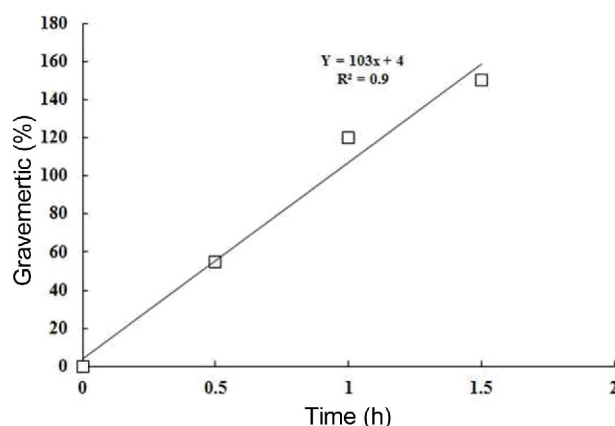


Figure 6. The change in weight percentage of grafted BC nanofibers (BC-MI-3-g-PHEMA) as a function of grafting reaction time.

Table 4. Gravimetric analysis results for changes in weight percentages of grafted BC nanofibers (BC-MI-3-g-PHEMA) at different reaction times

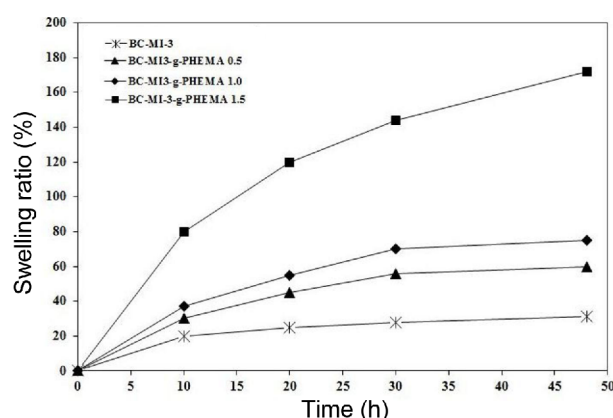
Samples	H ₂ O+BC (ml)	HEMA (ml)	CuCl (mg)	CuBr ₂ (mg)	bpy (mg)	Reaction time (h)	Sample dry weight (mg)	G* (%)
BC-MI-3	-	-				0	30	-
BC-MI-3-g-PHEMA-0.5	15	15	103.1	67.5	457.5	0.5	47	56.7
BC-MI-3-g-PHEMA-1	15	15	103.1	67.5	457.5	1	67	123.3
BC-MI-3-g-PHEMA-1.5	15	15	103.1	67.5	457.5	1.5	76	153.3

*G (%): weight of BC grafted with PHEMA relative to the weight of unreacted BC macroinitiator.

of grafting reaction time. A linear fit would indicate that there was a controlled polymerization process, however gravimetric analysis is not sufficient to confirm the controlled/living nature of ATRP [32]. Further examination of Figure 6 reveals that logarithmic fit would most likely represent the present system. This can be due to many constraints such as the short reaction time combined with the diffusion limitations for both catalyst and monomer imposed by the particle-like nature of BC shreds. This would yield longer graft polymer chains on the outside, and shorter graft polymer chains on the inside of a BC shred. In this case, the utilization of a more effective mixing technique at the beginning of the reaction would help to obtain a linear fit to results in Figure 6. This trend is similar to the study conducted by Kalial *et al.* [33] who studied the surface modification of natural fibers through chemical treatments. In their study, they examined different reaction parameters such as monomer concentration, reaction time and types of catalysts to achieve maximum grafting of ethyl acrylate on the sunn hemp fibers.

A fit linear equation is consistent with the gravimetric measurements obtained by Carlmark and Malmstrom [19] for poly(methyl acrylate) (PMA) grafted filter paper by ATRP. After 1 hour of reaction time, the weight of BC was doubled, while the maximum increase in the weight of filter paper was approximately 20 %.

Swelling analysis was performed to evaluate the water retention ability of the BC-MI-3 and the PHEMA grafted samples. The change in the swelling ratio percentages of the BC-MI-3 nanofibers (as a reference) and BC-MI-3-g-PHEMA-1.5 are presented in Figure 7. After a relatively fast water uptake during the first hour, the water absorption slightly decrease, which is leading gradually to a plateau behavior after 24 hours. However, the BC-MI-3-g-PHEMA-1.5 showed a considerably highest swelling ratio based on reaction time, specifically 144 % and 172 % after 30 hour and 48 hours, respectively. This is attributed to the BC amorphous regions with an enhance the grafting efficiency. The increase in grafting reaction time affects positively on the swellability of BC grafted PHEMA [21,22]. Moreover, the hydrolyzed grafted samples contained the hydrophilic functional group (-COOH), which increased the swelling and water uptake for polymer grafted nanofibers. Therefore, the PHEMA retained in the BC is strictly related to the

**Figure 7.** Change in swelling ratio of BC macroinitiator (BC-MI-3) and its grafted sample (BC-MI-3-g-PHEMA-1.5) as a function of time.

improvement in the swelling ratio [23,34]. This trend is an agreement with a functional groups that shown on FTIR analysis. The increased water retention capacity of the modified BC grafted with PHEMA would find several biomedical applications such as wound healing and topical drug delivery.

Thermogravimetric analysis was carried out as a function of reaction time (at 0.5, 1.0, and 1.5 hours) to evaluate the thermal stability and degradation profile of grafted BC nanofibers with respect to BC-MI-3 as a reference. The relationships between residual weights with temperatures are shown in Figure 8(A). The thermal stability is quite an important aspect in several applications. This includes applications when materials are exposed to high temperatures such as during sterilization process of biomedical materials. As shown in Figure 8(B), slight degradation was observed at 100 °C and continued to a maximum temperature of 400 °C. The PHEMA grafted nanofibers were consistently less stable than BC-MI-3 as degradation was clearly observed at 200 °C while it was observed for the non-grafted BC-MI-3 reference sample at 300 °C. Furthermore, the amount of loss in nanofibers' weights due to degradation increased in Figure 8 as PHEMA' grating increased. These results demonstrated that introducing of PHEMA grafts had a negative impact on the thermal stability of BC nanofibers that led to increasing

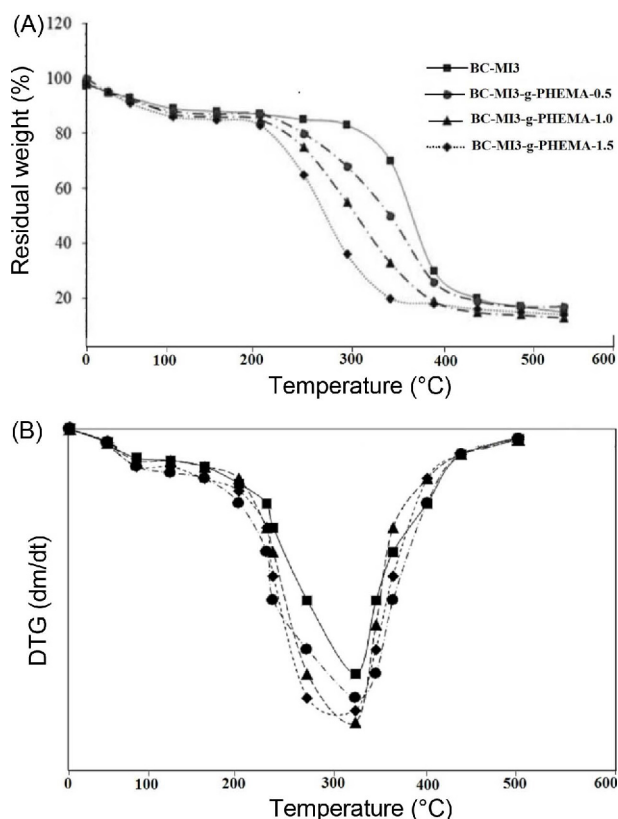


Figure 8. The change in residual weight of BC macroinitiator (BC-MI-3) and its grafted samples at different temperatures.

the degradation in general. The temperature at 20 % residual weight loss (T_{20}) slightly decreased from 335 °C for the ungrafted BC-MI-3 to 220 °C after grafting (i.e., BC-MI-3-g-PHEMA-1.5). This can be attributed to the hydrophilic nature of the PHEMA grafted chains. Accordingly, total weight loss at 550 °C decreased with increasing PHEMA chains grafted on the nanofibers (Figure 8(A)) [35].

T_{onset} , T_{max} and T_{50} of the BC-MI-3 and its grafted samples are summarized in Table 5. As shown in Table 5, the decomposition temperature at the 50 % weight loss (T_{50}) of the reference non-grafted nanofibers (BC-MI-3) occurs at 370 °C and rapidly decreased until 350 °C for the other samples of higher grafted percentages. In addition, the onset degradation temperature (T_{onset}) of the pristine sample (BC-

MI-3) is higher than that of the grafted samples. As can be observed in Table 5, the non-grafted sample BC-MI-3 has T_{max} of 390 °C, which decreased to 350 °C as a function of increasing PHEMA grafts contents. This confirms that introducing the PHEMA grafts resulted in decreasing the thermal stability of the nanofibers. Moreover, increasing graft reaction time has led to increasing the length of grafted polymer branches, which weakens the network structure of the polymer matrix [36]. The decrease in thermal stability of grafted nanofibers has been reported previously in the literature for cellulose substrates and lignocellulosic materials. This has been attributed to the degradation of bromoalkyl groups that induces cellulose degradation at lower temperatures [37]. In a previous work, Paula *et al.* [38], prepared nanocomposites of BC membranes grafted with acrylic polymers through ATRP. Similarly, they observed that the introduction of polymer grafts resulted in a decrease in the thermal stability of the BC fiber membrane.

Conclusion

ATRP is an effective technique for designing and preparing multifunctional, nanostructured materials for a variety of applications in biology and medicine. In the present work, BC macro-initiators were prepared by the reaction of the hydroxyl group of cellulose with various concentrations of 2-BiBr, followed by ATRP technique. The immobilization of 2-BiBr on the surface of BC was further confirmed by gravimetric measurement, which showed a slight linear increase in weight as the reaction time increased. The grafting of PHEMA was also confirmed by FTIR and EDS analyses. The PHEMA grafted BC nanofibers had a significantly higher swelling ratio than ungrafted nanofibers. Furthermore, the change in the swelling ratio percentages of the grafted nanofibers improved with increasing reaction time. TGA results revealed that the decomposition temperature at 50 % weight loss (T_{50}) decrease at 350 °C for the grafted nanofibers (i.e., BC-MI-3-g-PHEMA-1.5), while remarkably increased at 370 °C for (BC-MI-3) nanofibers. Subsequently, the results of this study present the successful use of BC nanofiber as a host for grafting acrylic monomers such as PHEMA by employing controlled radical polymerization techniques. Further, the effect of the hydrophilic/hydrophobic behavior of BC nanofibers can be tailored through the use of controlled/

Table 5. Thermal stability of BC macroinitiator (BC-MI-3) and its grafted samples at different reaction times

Polymer	T_{onset} (°C)	T_{20} (°C)	T_{50} (°C)	T_{max} (°C)	Weight loss at T_{50} (%)	Weight loss at T_{max} (%)	Residual weight % at 550 °C
BC	245	296	327	330	34	27	4
BC-MI-3	290	335	370	390	38.0	42.0	18
BC-MI-3-g-PHEMA-0.5	270	265	345	370	36.0	38.0	16
BC-MI-3-g-PHEMA-1.0	250	240	340	375	34.0	39.0	13
BC-MI-3-g-PHEMA-1.5	255	220	350	350	37.0	37.0	11

living radical polymerization methods. This substantial study can be applied in a degradable hydrogel in drug delivery systems and biomedical applications.

Acknowledgments

This work was financially supported by Agriculture and Agri-Food Canada and the Faculty of Engineering and Architectural Science at Ryerson University in Toronto, Canada.

References

1. P. Yang and S. P. Armes, *Macro. Rapid. Comm.*, **35**, 242 (2014).
2. E. Malmstrom and A. Carlmark, *Polym. Chem.*, **3**, 1702 (2012).
3. G. P. R. Figueiredo, A. R. P. Figueiredo, A. Alonso-Varona, S. C. M. Fernandes, T. Palomares, E. Rubio-Azpeitia, A. Barros-Timmons, A. J. D. Silvestre, C. P. Neto, and C. S. R. Freire, *BioMed. Res. I.*, <http://dx.doi.org/10.1155/2013/698141> (2013).
4. K. L. Robinson, M. A. Khan, M. V. D. Banez, X. Wang, and S. P. Armes, *Macromole*, **34**, 3155 (2001).
5. B. Reining, H. Keul, and H. Höcker, *J. Polymer*, **43**, 3139 (2002).
6. D. Roy, J. T. Guthrie, and P. Sébastien, *Macromole*, **38**, 10363 (2005).
7. W. Al-Abdallah and Y. Dahman, *Biopro. Biosyst. Eng.*, **36**, 1735 (2013).
8. Y. Dahman in "Encyclopedia of Nanoscience and Nanotechnology", 6th ed., pp.459-479, American Scientific Publisher, California, 2009.
9. Y. Dahman, K. E. Jayasuriya, and M. Kalis, *Appl. Biochem. Biotech.*, **162**, 1647 (2012).
10. J. S. Wang and K. Matyjaszewski, *J. Am. Chem. Soc.*, **117**, 5614 (1995).
11. M. Kato, M. Kamigaito, M. Sawamoto, and T. Higashimura, *Macromole*, **28**, 1721 (1995).
12. B. Boutevin, *J. Polym. Sci.*, **38**, 3235 (2000).
13. P. Krol and P. Chmielarz, *eXPRESS Polym. Lett.*, **7**, 249 (2013).
14. T. Ameringer, F. Ercole, K. M. Tsang, B. R. Coad, X. Hou, A. Rodda, D. R. Nisbet, H. Thissen, R. A. Evans, L. Meagher, and J. S. Forsythe, *Bio-interphases*, **8**, 16 (2013).
15. T. E. Patten, J. Xia, T. Abernathy, and K. Matyjaszewski, *Science*, **272**, 866 (1996).
16. Y. Dahman and T. Oktem, *J. Appl. Polym. Sci.*, **126**, 188 (2011).
17. R. Alosmanov, K. Wolski, and S. Zapotoczny, *Cellulose*, **24**, 258 (2017).
18. W. Huang, J. B. Kim, M. L. Bruening, and G. L. Baker, *Macromole*, **35**, 1175 (2002).
19. A. Carlmark and E. Malmstrom, *Biomacromole*, **4**, 1740 (2003).
20. L. Bach, Q. Bui, X. Cao, V. Ho, and K. Lim, *Polym. Bull.*, **73**, 2627 (2016).
21. X. Shen, J. L. Shamsheina, P. Berton, G. Gurau, and R. D. Rogers, *Green Chem.*, **18**, 53 (2016).
22. Z. Wang, C. Crandall, V. L. Prautzsch, R. Sahadevan, T. J. Menkhaus, and H. Fong, *ACS Appl. Mat. Inter.*, doi: 10.1021/acsami.6b16116 (2017).
23. R. Endo, K. Yamamoto, and J.-I. Kadokawa, *J. Fibers*, **3**, 338 (2015).
24. N. J.-I. Kadokawa, *Coatings*, **6**, 27 (2016).
25. F. A. D. Santos, C. V. Gisele Iulianelli, and M. I. B. Tavares, *Mater. Sci. Appl.*, **7**, 257 (2016).
26. C. Verlhac and J. Dedier, *J. Polym. Sci.: Part A: Polym. Chem.*, **28**, 1171 (1990).
27. S. Corneillie and M. Smet, *Polym. Chem.*, **6**, 850 (2015).
28. D. Shen and Y. Huang, *Polymer*, **45**, 7091 (2004).
29. Aldrich Library of FTIR Spectra Aldrich Chemical Co., Chem. Lib. Ref., 66, pp.743-744, 1989.
30. L. Gang, Y. Haipeng, and L. Yixing, *Adv. Mater. Res.*, **221**, 90 (2011).
31. M. Pulat and F. Nuralin, *Cell Chem. Technol.*, **48**, 137 (2014).
32. S. K. Fierens, D. R. D'hooge, H. M. Van Steenberge, M.-F. Reyniers, and G. B. Marin, *Polymer*, **7**, 655 (2015).
33. S. Kalial, A. Kumar, and B. S. Kaith, *Adv. Mater. Lett.*, **4**, 742 (2013).
34. M. H. Casimiro, J. P. Leal, and M. H. Gil, *Nucl. Instr. Meth. Phys. Res. B*, **236**, 482 (2005).
35. M. Szuwarzyński, K. Wolski, and S. Zapotoczny, *Polym. Chem.*, **7**, 5664 (2016).
36. C. Boyer, N. A. Corrigan, K. Jung, D. Nguyen, T.-K. Nguyen, N.-N. M. Adnan, S. Oliver, S. Shanmugam, and J. Yeow, *Chem. Rev.*, **116**, 1803 (2016).
37. A. A. Singh and S. Palsule, *Compos. Interface*, **20**, 553 (2013).
38. S. S. Paula, A. Lacerda, M. M. V. Barros-Timmons, S. R. Carmen, J. D. Armando, and C. P. Neto, *Biomacromole*, **14**, 2063 (2013).